J. Automation & Systems Engineering 13-3 (2019): 93-105

Regular paper

Comparative Analysis of Advanced PWM Techniques and Various Multi-Level Inverters Applied to the Electric Vehicle System

Waad Rtibi, Lotfi M'braki, and Moez Ayad

Laboratory of Electronic Systems & Sustainable Energy (ESSE), University of Sfax, Tunisia

Abstract-This article proposes an Electric Vehicle (EV) system driven by the rotor-field-oriented control of the induction motor. In order to find the best-adjusted inverter for our EV system. We studied the output current and the torque behavior of various inverter types. These inverters are basically the classical inverter, the H-bridge inverter, and the Neutral Point Clamped (NPC) inverter. The multi-level inverter technique is applied on both H-bridge and the NPC inverter, as a result, we have the alteration between the energy levels in the inverters, such as three levels and five levels. The classical inverter is commanded by the pulse width modulation (PWM) technique. The three and five levels inverter are commanded by two derivate methods of the PWM which are the PDC-PWM technique (Phases Disposition Carrier- PWM) and the PSC-PWM technique (Phases Shifted Carrier- PWM). The main objective is to select the inverter that gives the system more stability, effectiveness, and autonomy. The energy consumption and the total harmonic distortion THD percentage are the main criteria to select the appropriate inverter. The article used MATLAB/SIMULINK to compare the nine inverters outcomes. And to choose the best inverter implemented in the suggested system.

Keywords: Electric vehicle (EV), induction motor (IM), field-oriented control (FOC), pulse width modulation (PWM), H-bridge inverter, NPC inverter.

1. NOMENCLATURE

R_s	Stator resistance (1.4534 Ω)
R_r	Rotor resistance (1.4160 Ω)
L_r	Rotor inductance (0.0143H)
L_s	Stator inductance (0.0144H)
M	Mutual inductance (0.0132H)
f	Friction coefficient (0.014 kg.m² /S)
j	Moment of inertia (0.311kg.m²)
p	Number of pole pairs in the motor (2)
ω_s	Synchronization angular speed
ω_m	Electromechanical angel speed of the motor
T_r	load of torque
s	Laplace operator

$Q = 1 - \frac{M^2}{L_s \times L_r}$ Total leakage factor

$\sigma_s = \frac{L_s}{R_s}$ Stator Time constant

$\sigma_r = \frac{L_r}{R_r}$ Rotor Time constant

2. INTRODUCTION

EV needs to find the greatest combination able to reduce toxic gases emission, reduce energy consumption, works longer time and improve its effectiveness. The motor selection is one very important factor that helps to reach this goal. IM is one of the naturally adoptions for EV applications. It is rugged and efficient, in addition, it needs less maintenance as compared with other machines. As well, it operates in difficult environments and at variable speed [1][2].

The motor is commanded by the field-oriented control (FOC), it is a control-strategy inspired by the DC motor control because it is easy to use due to its independence between the flux and torque. Which are decoupled and controlled separately [3], [4], [5].

The main energy source is the battery, in order to supply the IM, it needs to be adapted by mean of the inverter which converts the DC voltage to AC form. The most popular inverter used in EV manufacturing is the classical inverter. It is a great technique supporting low-power applications. But the EV needs a larger power consumption (high-power and medium-power). Besides, it is required to minimize the passive components in the current and voltage outputs and to increase the switching frequency in the semi-conductors to several kilohertz levels. Consequently, the EV applications provisions is a multi-level inverter to minimize the switching losses once increasing the switching frequencies [6]–[9].

The proposed EV design is formed by one IM, one battery feeding a multi-level inverter and the control system. Several multi-level inverter categories are introduced with the intention to discover the greatest one to use in the proposed EV system. The first inverter topology is the H-bridge. It decreases the energy losses in switches commutation. Besides, it diminishes the THD percentage in the inverter. The second one is the NPC inverter. It is developed to give energy conversion more advantages, several voltage levels, and fewer losses. It saves energy, and, it reduces the power consumption in the switches by minimizing the THD%.

Certainly, energy management involves the inverter development, the system have to be more organized in order to increase the active period of the EV. Therefore, both topologies H-bridge and NPC are tested in the three-level and five-level strategies. The semiconductor switching is commended by the PWM command. It delivers a wave of the impulse towards IGBTs to make it commute successively. The sinusoidal modulator (low-frequency) is compared to the triangular carriers (high-frequency) to create the PWM command. In fact, the position of the carriers creates different PWM techniques [10]. The PDC-PWM and the PSC-PWM strategies are tested and applied to the inverters. The inverters described before can be summarized in nine categories, they are as follows, i) Classical inverter, ii) Three-level PSC-PWM H-bridge, iii) Three-level PDC-PWM H-bridge, iv) Five-level PSC-PWM H-bridge, v) Five-level PDC-PWM H-bridge, vi) Three-level PSC-PWM NPC, vii)Three-level PDC-PWM NPC, viii) Five-level PSC-PWM NPC, ix) Five-level PDC-PWM NPC.

The following parts of the paper are organized as follows. Section 3 investigates the

different studied inverters natures: i) the classical inverter, ii) the three-level and five-level H-bridge inverter, iii) the three-level and five-level NPC inverter. Section 4 examines the PWM command (PSC-PWM and PDC-PWM). The mathematical modulation of the FOC-IM is presented in section 5. The simulation results obtained by MATLAB/SIMULINK are analyzed in Section 6, the proposed system compare the nine inverter-topologies proposed for the EV propulsion applications. To finish, the conclusion is presented in Section 7.

3. MULTI-LEVEL INVERTER

The insulated gate bipolar transistors (IGBT) is characterized by its high voltage and high current grades. In case of short-circuit currents, the IGBT is designed to function for more than 10µs. Besides, it is reliable and lives-long. Therefore, the IGBT is used as the power device in various inverters, particularly, in the EV design [11]–[13].

The inverter is used in the EV system to convert power from the batteries exit (DC) to the IM input (AC). This offers power abilities and efficiency for the electrical system. The inverter chosen structure will make a very important difference in power management. It highly influences the output current and voltage stress, and THD percentage. Consequently, it effects the stress in the motor behaviors. The number and the order of IGBTs in an inverter create different inverter types [2],[12].

3.1. Classical

The classical three-phase inverter is presented in figure 1. It is formed by six IGBTs. IGBTs commute simultaneously to create a three-level voltage. This structure needs amelioration because the THD is high.

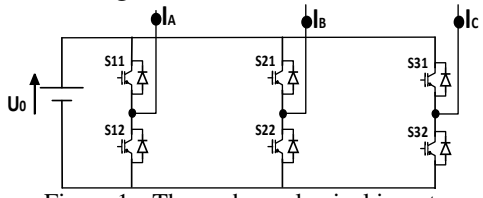

Figure 1. Three-phase classical inverter

Equation (1) express the voltage of the classical inverter. The continuous source is designed by (U_0), S_{ij} presents the IGBT order (i ∈ {1,2,3}is the phase order, j ∈{1,2} is the IGBT number in the same phase).

$$\begin{bmatrix} V_A \\ V_B \\ V_C \end{bmatrix} = \frac{U_0}{3} \begin{bmatrix} 2 & -1 & -1 \\ -1 & 2 & -1 \\ -1 & -1 & 2 \end{bmatrix} \begin{bmatrix} S_{11} \\ S_{21} \\ S_{31} \end{bmatrix} \quad (1)$$

3.2. Three-level H-bridge inverter

The three-level H-bridge inverter (figure 2) is designed by one continuous source (V_c) connected to four IGBTs in H form to produce an alternative output voltage with the three levels voltage {-V_c, 0, +V_c}.

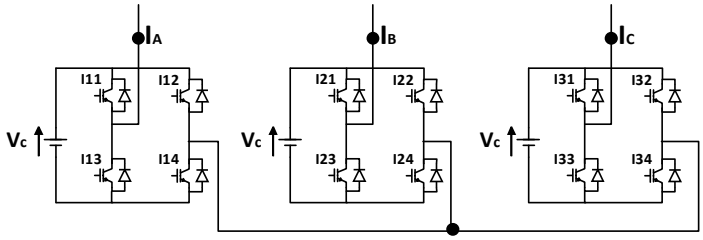

Figure 2. Three-phase, three-level H-bridge inverter

Equation (2) shows the voltage of the three-level H-bridge inverter. I_{ij} presents the IGBT order in the H-bridge inverter (i ∈{1,2,3}is the phase number and j ∈{1,2,3,4} is the IGBT rank in the same cell).

$$\begin{bmatrix} V_A \\ V_B \\ V_C \end{bmatrix} = \frac{V_C}{3} \begin{bmatrix} 2 & -1 & -1 \\ -1 & 2 & -1 \\ -1 & -1 & 2 \end{bmatrix} \begin{bmatrix} I_{11} + I_{14} - 1 \\ I_{21} + I_{24} - 1 \\ I_{31} + I_{34} - 1 \end{bmatrix} \tag{2}$$

3.3. Five-level H-bridge inverter

A five-level H-bridge inverter is made by two cells. In fact, each cell is already three-level H-bridge inverter. The output voltage levels are respectively {+2V_c, + V_c, 0, - V_c, - 2V_c}. These modifications generate an output voltage which is more comparable to the sinusoidal waveform to reduce the THD value. Figure 3 presents the five-level H-bridge inverter [14].

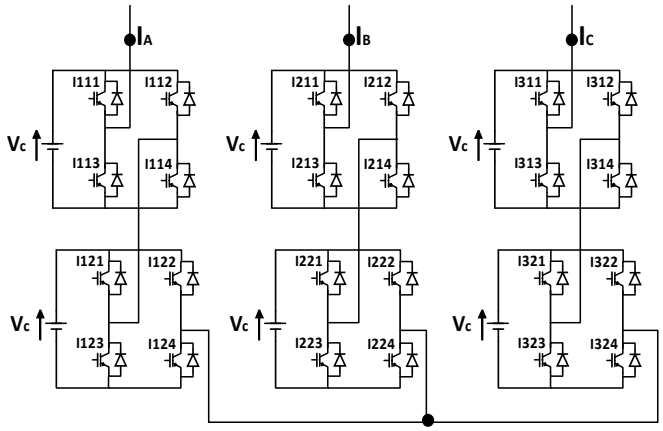

Figure 3. Three-phase, five-level H-bridge inverter

The voltage of the five-level H-bridge inverter is presented in equation (3) with I_{ijk} presents the IGBT order in the H-bridge inverter (i ∈{1,2,3}is the phase number, j ∈{1,2} is the cell number and k ∈{1,2,3,4} is the IGBT rank in the same cell).

$$\begin{bmatrix} V_A \\ V_B \\ V_C \end{bmatrix} = \frac{V_C}{3} \begin{bmatrix} 2 & -1 & -1 \\ -1 & 2 & -1 \\ -1 & -1 & 2 \end{bmatrix} \begin{bmatrix} (I_{111} + I_{114} - 1) + (I_{121} + I_{124} - 1) \\ (I_{211} + I_{214} - 1) + (I_{221} + I_{224} - 1) \\ (I_{311} + I_{314} - 1) + (I_{321} + I_{324} - 1) \end{bmatrix} \tag{3}$$

3.4. Three-level NPC inverter

The three-level NPC inverter (figure 4) is designed by one continuous source (V_{dc}) serving four IGBTs and two diodes taken up in anti-parallel line to produce an AC output voltage. A voltage divisor formed by two condensers C_1 and C_2 (we propose that C_1 and C_2

are uniforms) is connected parallel to the DC source. It produces three voltage levels {+V_{dc}, 0, -V_{dc}} [15].

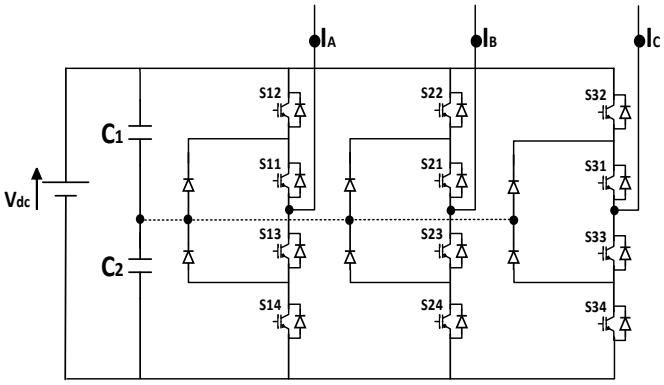

Figure 4. Three-phase, three-level NPC inverter

Equation (4) express voltage of the three-level NPC inverter we need to define S_{ij}, it is the IGBT order in the inverter (i ∈{1,2,3} phase number, j ∈[1 4] IGBT rank in the same phase) [16]. We note that V_{dc1} and V_{dc2} are respectively the voltage of the capacitor C_1 and C_2.

$$\begin{bmatrix} V_A \\ V_B \\ V_C \end{bmatrix} = \frac{1}{3}\begin{bmatrix} 2 & -1 & -1 \\ -1 & 2 & -1 \\ -1 & -1 & 2 \end{bmatrix}\left\{\begin{bmatrix} K_{1m} \\ K_{2m} \\ K_{3m} \end{bmatrix} V_{dc1} - \begin{bmatrix} K_{1n} \\ K_{2n} \\ K_{3n} \end{bmatrix} V_{dc2}\right\} \tag{4}$$

$$\text{With } \begin{cases} K_{im} = S_{i1} \times S_{i2} \\ K_{in} = S_{i3} \times S_{i4} \end{cases}$$

3.5. Five-level NPC inverter

The five-level NPC inverter is formed by eight IGBTs connected to six protection diodes. And it is fed by a main continuous voltage (V_{dc}). The output voltage levels are {+2V_{dc}, + V_{dc}, 0, - V_{dc}, -2V_{dc}}. These modifications generate an output voltage which is more similar to the sinusoidal waveform to reduce the THD value. Figure 5 presents the five-level NPC inverter [17].

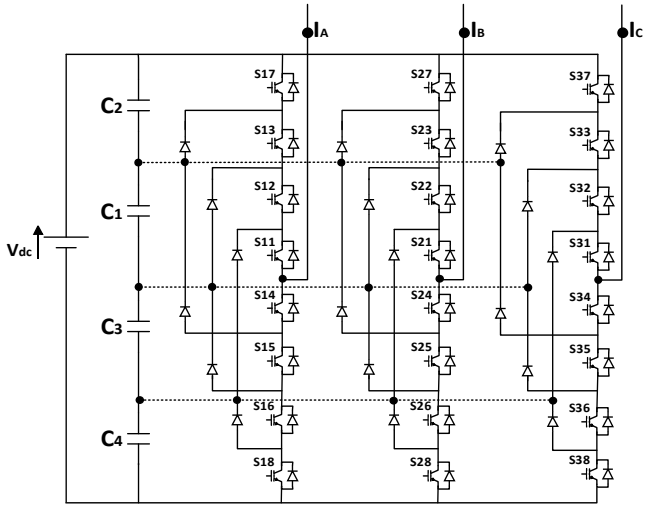

Figure 5. Three-phase, five-level NPC inverter

The voltage in the five-level NPC inverter is presented in equation (5). S_{ij} expresses the IGBT order in the inverter (i ∈{1,2,3} phase number, j ∈[1 8] IGBT rank in the same cell).

And we propose that all the capacitors C_1, C_2, C_3, and C_4 are uniform, [18]–[20].

$$\begin{bmatrix} V_A \\ V_B \\ V_C \end{bmatrix} = \frac{1}{3}\begin{bmatrix} 2 & -1 & -1 \\ -1 & 2 & -1 \\ -1 & -1 & 2 \end{bmatrix}\begin{bmatrix} 2K_{1m} + S_{17} - 2K_{1n} - S_{18} \\ 2K_{2m} + S_{27} - 2K_{2n} - S_{28} \\ 2K_{3m} + S_{37} - 2K_{3n} - S_{38} \end{bmatrix} V_{dc} \tag{5}$$

$$\text{With } \begin{cases} K_{im} = S_{i1} \times S_{i2} \times S_{i3} \\ K_{in} = S_{i4} \times S_{i5} \times S_{i6} \end{cases}$$

4. THE PWM STRATEGY

In the previous section, we have studied the multilevel inverter type H-bridge then type NPC, which allow the creation of multi-level voltage and current. The aim of this study is to reduce the THD percentage of the voltage and the current at the inverter output [21].

The command strategy is one very important factor that helps to save energy. Therefore, it is important to be attentive to the strategy chosen. The DC input voltage is transformed into an AC output voltage by means of the PWM inverter. Actually, the PWM is a suitable command strategy used in the high power conversion area. It gives an effective power conversion and low energy losses.

A high-frequency signal commands the IGBTs commutation. This command signal is resulting by comparing the low-frequency sinusoidal signal, called modulator, with the high-frequency triangular signals. This command generates a reduced harmonic in the output current and voltage [10].

The modulator amplitude (M_i) index is 0,9 V, and its frequency (F_m) is equal to 60 Hz, it is multiplied by the fundamental frequency (f) to provide the carrying frequency (F_p) as shown in equation (6) [22]–[24].

$$F_p = F_m \times f \tag{6}$$

The THD percentage is a very important factor that helps to make a good chose. It is calculated by equation (7), the symbol X is the voltage or the current.

$$THD_x\% = \sqrt{\frac{\sum_{n=2}^{\infty} X_{nRMS}^2}{X_{1RMS}^2}} 100\% \tag{7}$$

The high-frequency triangular signals are called carriers. Its number, amplitude, and phase are very important to recognize the PWM command type. The number of carriers is selected by the inverter type. Starting with one carrier (Figure 6), it is used to command the classical inverter, two carriers are used to command three level inverters and four carriers are used to command five level inverters. The way the carriers are varied between them gives born to different PWM types. In this paper, two types are studied the PDC-PWM and the PSC-PWM.

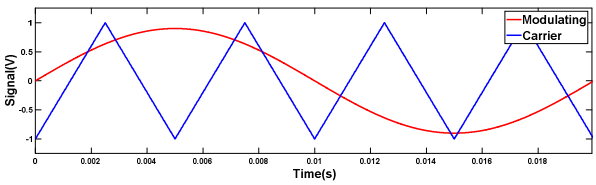

Figure 6. PWM command modulator sinusoidal signal and triangular carrier

4.1. PDC-PWM command

The PDC-PWM is resulting by vertically moving the carriers, that is to say, equally dividing the interval [-1 1] between them. If the commanded inverter is a three-level one, there will be two carriers that have the amplitudes [-1 0] and [0 1] and, if it is a five-level inverter, there will be four carriers that have the amplitudes [-1 -0.5], [-0.5 0], [0 0.5] and [0.5 1]. Figure 7 shows the PDC-PWM command.

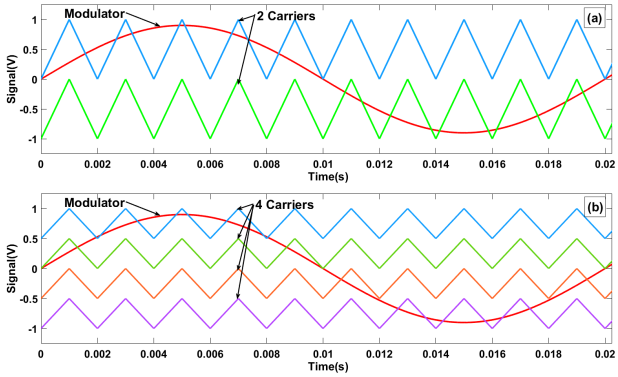

Figure 7. PDC-PWM command: a) three-level command. b) five-level command.

4.2. PSC-PWM command

The second command is the PSC-PWM. Its carriers are horizontally shifted comparative to the time axis. Carriers phase are distributing the interval [0 2π]. The three-level inverter is commanded by two carriers having the phases [0 π], [π 2π] and the five-level one has four carriers taking phases as [0 π/2], [π/2 π], [π 3π/2] and [3π/2 2π]. Figure 8 shows the PSC-PWM command.

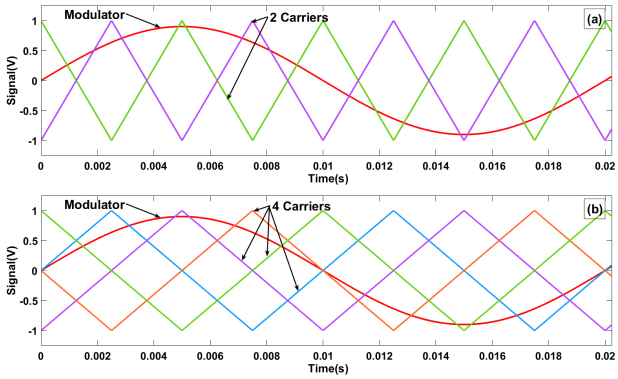

Figure 8. PSC-PWM command: a) three-level command. b) five-level command.

5. A MATHEMATICAL MODEL OF THE INDUCTION MOTOR

The IM is largely used in the electric vehicle domain. It is able to work in difficult environments at different speeds, as driver requests. It is developed after many engineering studies. Whereas, the torque and the flux are dependent consequently, the system control is needed to overcome this complexity [25]. The FOC-IM makes the IM control easier by analogy with the DC motor. The FOC-IM design is collected by Park modulation an Estimator which lets determining torque, flux and speed values: T_e, φ_r, and ω. The system stability requires to have a torque regulator and a flux regulator [2], [26]–[28].

Equation (8) shows the d-axis stator voltages V_{ds}. Then equation (9) expresses the q-axis stator voltages V_{qs}. The direct component of stator current I_{ds} is related to the rotor flux

level φ_r and the indirect stator current I_{qs} is related to the electromagnetic torque T_{em} as presented in equations (10) and(11) [26], [29]. The flux and the electromagnetic torque are presented respectively in equations (12) and (13)

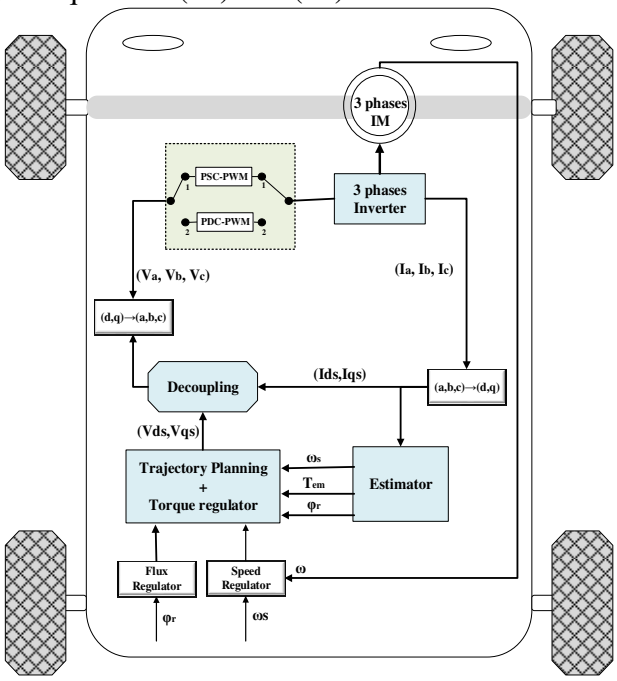

Figure 9. Plan of the rotor FOC-IM of EV

$$V_{ds} = R_s Q \sigma_s \left[\frac{dI_{ds}}{dt} + \frac{1}{Q\sigma_s} I_{ds} - \omega_s I_{qs} + \frac{(1-Q)}{MQ} \frac{d\varphi_r}{dt} \right] \tag{8}$$

$$V_{qs} = R_s Q \sigma_s \left[\frac{dI_{qs}}{dt} + \frac{1}{Q\sigma_s} I_{qs} + \omega_s I_{ds} + \frac{(1-Q)}{MQ} \omega_s \varphi_r \right] \tag{9}$$

$$I_{ds} = \frac{\sigma_r}{M} \left(\frac{d\varphi_r}{dt} + \frac{\varphi_r}{\sigma_r} \right) \tag{10}$$

$$I_{qs} = \frac{L_r}{pM\varphi_r} T_{em} \tag{11}$$

$$\varphi_r = \frac{M}{1+\sigma_r . s} I_{ds} \tag{12}$$

$$T_{em} - T_r = f \frac{\omega_m}{p} + \frac{j}{p} \frac{d\omega_m}{dt} \tag{13}$$

Figure 9 displays the proposed structure, the IM equation are referenced by the d-q model. It is connected to the bloc Park modulation and its opposite (inv-Park modulation). It is coupled to an inverter by means of the PWM command. The estimator block calculates the torque, flux and speed values. It is required to have a torque and flux regulators to

guarantee the system stability. And a decoupling bloc is used to separate the torque and flux component [2][5].

With the intention of making the EV moves easily restored by the Total traction force F_T (equation (14)), it is needed that the totality of the powertrain four forces (F_r, F_a, F_p, and F_{ac}) overcomes the vehicle movement [2], [7], [30].

$$F_T = F_r + F_{pr} + F_a + F_{ac} \tag{14}$$

With

F_r: The rolling resistance force

F_{pr}: The road profile force

F_a: The aero-dynamic resistance force

F_{ac}: The acceleration force

6. SIMULATION AND DISCUSSION

The proposed system is tested by MATLAB/SIMULINK, it presents the FOC-IM, powered via a multi-level inverter for the EV application. The PDC-PWM and PSC-PWM output command are shown in the figures 10 and 11, respectively.

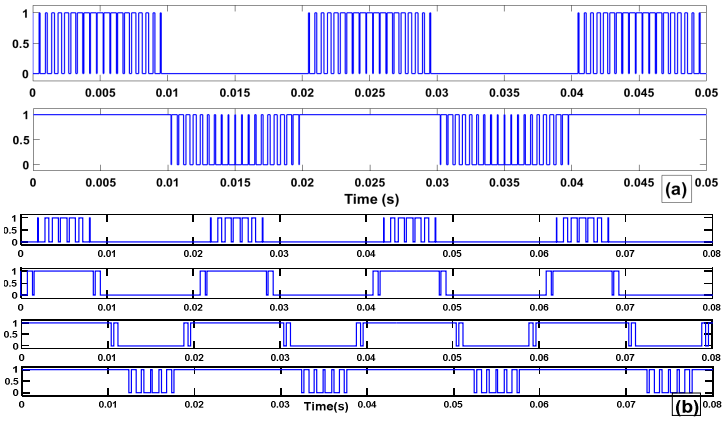

Figure 10. PDC-PWM output command: a) three-level command. b) five-level command.

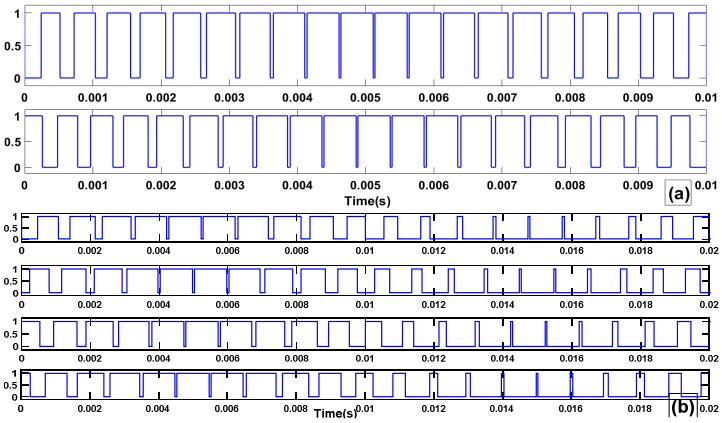

Figure 11. PSC-PWM output command: a) three-level command. b) five-level command.

Nine different inverters are simulated and compared between them in order to find the best inverter for this system. Each inverter output is shown in one window of the figures to clarify the differences.

In figure 12 nine windows are displayed. They present the output current of each inverter. The classical and the three-level NPC inverter as same as the three-level H-bridge inverter give an output current approximately equal to 59A and the THD_I is over1.1%. The

five-level NPC inverter has an unstable output current.

The five-level H-bridge inverter output current is equal to 57A. The THD_I is 1.12 % when the command is the PSC-PWM and it is 0.74% with the PDC-PWM command.

The most appropriate inverter is clearly the five-level PDC-PWM H-bridge inverter. Since the output voltage shows the same behavior as the current as shown in Table I.

According to the electromagnetic torque presented in figure 13 the system feed by the five-level H-bridge inverter is the most appropriate one to convert energy into this system because it follows the instruction and it is stable. The PDC-PWM presents a better THD % then the PSC-PWM.

Table 1 summarizes the system results from the nine tested inverters. Both THD_I and THD_V shows the same attitude, theirs values are very highs in the classical inverter, the three-level H-bridge inverters and the PSC-PWM three-level NPC inverter. They are smaller in the rest. And it shows an excellent answer to the system needs in the PDC-PWM five-level H-bridge inverter.

TABLE I. SUMMARY RESULTS OBTAINED BY THE NINE INVERTERS

Inverter	Current (A)	THD_I %	Voltage (V)	THD_V %	Torque (Nm)
Classical inverter	59.8	2.77	227	59.8	60
PDC-PWM 3 levels H	58.9	1.15	225	49.1	60
PSC-PWM 3 levels H	58.8	1.5	225	50.1	60
PDC-PWM 3 levels NPC	59.7	1.0	226	52.1	60
PSC-PWM 3 levels NPC	59.8	2.47	227	55.4	60
PDC-PWM 5 levels H	57.6	0.74	223	12.3	60
PSC-PWM 5 levels H	57.7	1.12	224	25.8	60
PDC-PWM 5 levels NPC	59	0.25	220	20.1	60
PSC-PWM 5 levels NPC	59.5	1.76	227	36.7	60

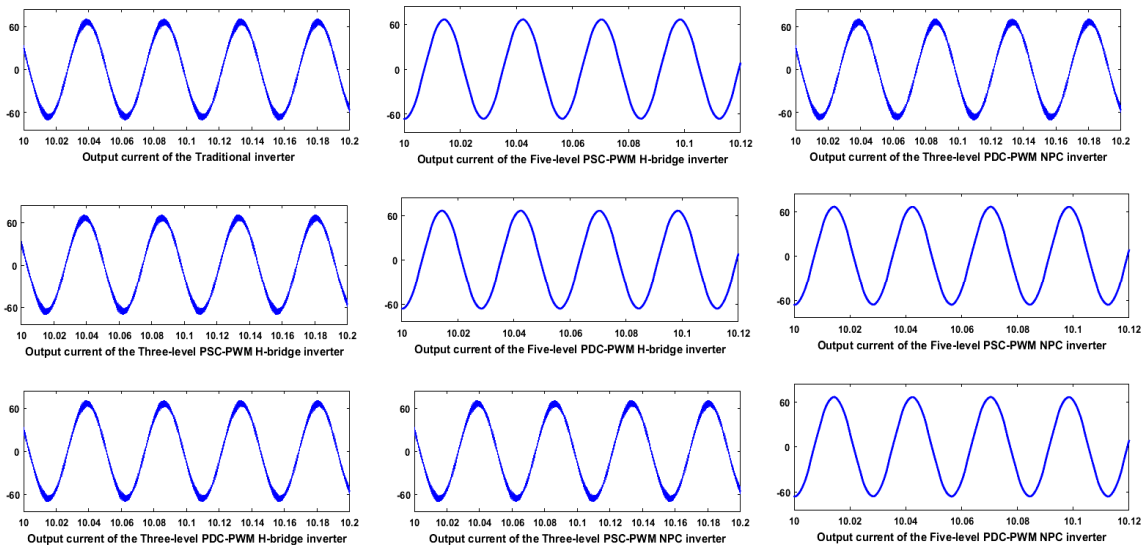

Figure 12. The output current I_A of the IM-inverter

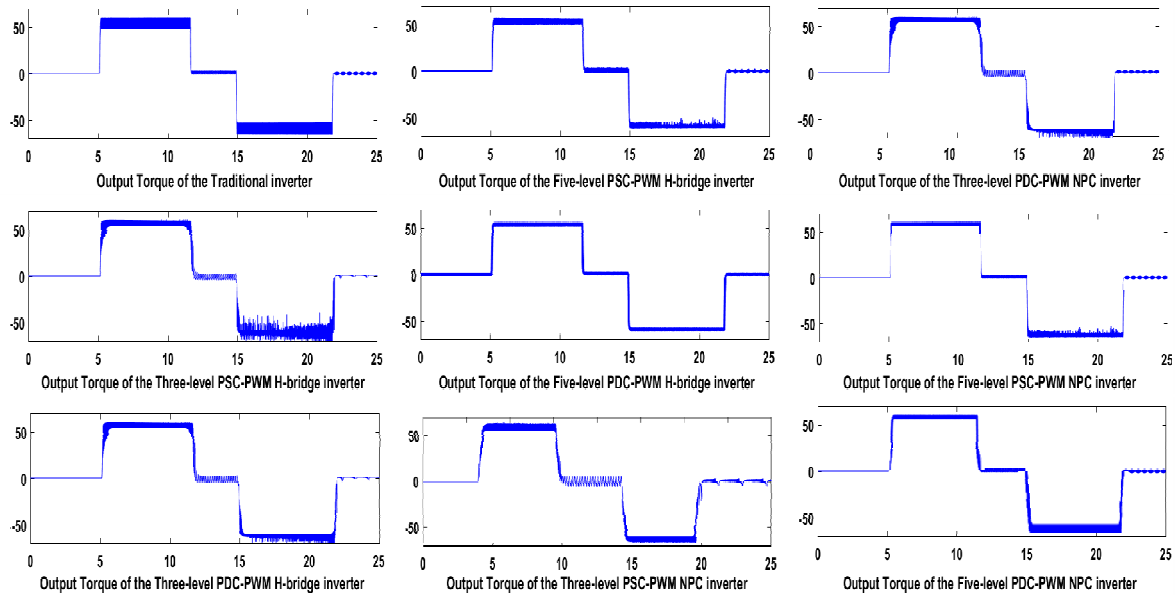

Figure 13. The electromagnetic torque of the IM-inverter

7. CONCLUSION

In this article, a comparative study was analyzed, nine inverters were proposed to be implemented in the EV system. The use of a worthy method guarantees the best organization of the system. The FOC-IM is supported by the PWM command strategy of the multi-level inverter. A special interest was given to improve the EV stability by the good chose of the system components. The inverters were alternated by varying its command strategy, its power density (voltage-level) and its form; these factors help to create nine diverse inverters. The inverter development allows improving the robustness and stability of the EV, to decrease energy losses in semiconductors commutation by reducing THD %. The simulation shows a good response in the five-level H-bridge inverter, especially, with the PDC-PWM command.

ACKNOWLEDGMENT

We would like to thank the University of Sfax-Tunisia, and National School of Engineers of Sfax, Laboratory of Electronic Systems & Sustainable Energy (ESSE), and Electric Transport Base of STEG-Gafsa Tunisia for providing the research facilities.

REFERENCES

[1] A. Ltifi, M. Ghariani, M. Ayadi, and R. Neji, “A sliding mode integrated control technique and the PI regulator for induction machine,” J. Electr. Syst., vol. 12, no. 4, pp. 801–816, 2016.

[2] S. M. E. Fadul, I. B. Aris, N. Misron, I. A. Halin, and A. K. M. Iqbal, “Modelling and Simulation of Powertrain System for Electric Car,” J. Soc. Automot. Eng. Malaysia, vol. 2, no. 1, pp. 23–34, 2018.

[3] V. S. S. Pavan Kumar Hari, A. Tripathi, and G. Narayanan, “Experimental determination of mechanical parameters in sensorless vector-controlled induction motor drive,” Sadhana - Acad. Proc. Eng. Sci., vol. 42, no. 8, pp. 1285–1297, 2017.

[4] F. L. Mapelli, D. Tarsitano, and F. Cheli, “MRAS rotor resistance estimators for EV vector controlled induction motor traction drive: Analysis and experimental results,” Electr. Power Syst. Res., vol. 146, pp. 298–307, 2017.

[5] J. Lara and A. Chandra, "Performance investigation of two novel HSFSI demodulation algorithms for encoderless FOC of PMSMs intended for EV propulsion," IEEE Trans. Ind. Electron., vol. 65, no. 2, pp. 1074–1083, 2017.

[6] S. Mukherjee, S. Kumar Giri, S. Kundu, and S. Banerjee, "A generalized discontinuous PWM scheme for three-level NPC traction inverter with minimum switching loss for electric vehicles," IEEE Trans. Ind. Appl., vol. 55, no. 1, pp. 516–528, 2019.

[7] M. Ehsani, Y. Gao, S. Longo, and K. M. Ebrahimi, Modern Electric, Hybrid Electric, and Fuel Cell Vehicles, Third Edit. CRC Press Taylor & Francis Group, 2018.

[8] L. Dorn-Gomba, P. Magne, B. Danen, and A. Emadi, "On the Concept of the Multi-Source Inverter for Hybrid Electric Vehicle Powertrains," IEEE Trans. Power Electron., vol. 33, no. 9, pp. 7376–7386, 2018.

[9] B. Kirankumar, Y. V. Siva Reddy, and M. Vijayakumar, "Multilevel inverter with space vector modulation: Intelligence direct torque control of induction motor," IET Power Electron., vol. 10, no. 10, pp. 1129–1137, 2017.

[10] P. S. V Kishore and P. S. Kumar, "Comparison of Multi Carrier PWM Techniques applied to Five Level CHB Inverter," Int. J. Pure Appl. Math., vol. 114, no. 7, pp. 77–87, 2017.

[11] K. K. Gupta, A. Ranjan, P. Bhatnagar, L. K. Sahu, and S. Jain, "Multilevel inverter topologies with reduced device count: A review," IEEE Trans. Power Electron., vol. 31, no. 1, pp. 135–151, 2016.

[12] T. M. Jahns and H. Dai, "The Past , Present , and Future of Power Electronics Integration Technology in Motor Drives," CPSS Trans. Power Electron. Appl., vol. 2, no. 3, pp. 197–216, 2017.

[13] A. Choudhury, P. Pillay, and S. S. Williamson, "DC-bus voltage balancing algorithm for three-level Neutral-Point-Clamped (NPC) traction inverter drive with modified virtual space vector," IEEE Trans. Ind. Appl., vol. 52, no. 5, pp. 3958–3967, 2016.

[14] P. Thongprasri, "A 5-Level Three-Phase Cascaded Hybrid Multilevel Inverter," Int. J. Comput. Electr. Eng., vol. 3, no. 6, pp. 789–794, 2011.

[15] M. Schaefer, W. Uas, M. Hofmann, W. Uas, S. Raab, and A. Ackva, "FPGA based control of an three level neutral point clamped inverter," in PCIM Europe 2017 - International Exhibition and Conference for Power Electronics, Intelligent Motion, Renewable Energy and Energy Management, 2017, no. May, pp. 16–18.

[16] H. Boumaaraf, A. Talha, and O. Bouhali, "A three-phase NPC grid-connected inverter for photovoltaic applications using neural network MPPT," Renew. Sustain. Energy Rev., vol. 49, pp. 1171–1179, 2015.

[17] "Simulation and Modeling of a Five -Level (NPC) Inverter Fed by a Photovoltaic Generator and Integrated in a Hybrid Wind-PV Power ... Simulation and Modeling of a Five -Level (NPC) Inverter Fed by a Photovoltaic Generator and Integrated in a Hybrid Win," Eng. Technol. Appl. Sci. Res., no. September, 2017.

[18] J. Falck, C. Felgemacher, A. Rojko, M. Liserre, and P. Zacharias, "Reliability of Power Electronic Systems," IEEE Ind. Electron. Mag., vol. 12, no. 2, pp. 24–35, 2018.

[19] B. Wu and M. Narimani, "Diode-Clamped Multilevel Inverters," in High-Power Converters and AC Drives, John Wiley & Sons, Inc, 2017.

[20] M. Rezki and I. Griche, "Simulation and Modeling of a Five -Level (NPC) Inverter Fed by a Photovoltaic Generator and Integrated in a Hybrid Wind-PV Power System.," Eng. Technol. Appl. Sci. Res., vol. 7, no. 4, pp. 1759–1764, 2017.

[21] M. M. Biswas and M. Z. R. Khan, "Amended THD with modified phase-shifted PWM for micro-grid connected multilevel inverter," 2017 IEEE Power Energy Conf. Illinois, PECI 2017, no. 1, 2017.

[22] D. L. Mon-Nzongo, T. Jin, G. Ekemb, and L. Bitjoka, "Decoupling Network of Field-Oriented Control in Variable-Frequency Drives," IEEE Trans. Ind. Electron., vol. 64, no. 7, pp. 5746–5750, 2017.

[23] V. Sonti, S. Jain, and S. Bhattacharya, "Analysis of the modulation strategy for the minimization of the leakage current in the PV grid-connected cascaded multilevel inverter," IEEE Trans. Power Electron., vol. 32, no. 2, pp. 1156–1169, 2017.

[24] S. Pramanick, R. S. Karthik, N. A. Azeez, K. Gopakumar, S. S. Williamson, and K. S. Rajashekara, "A harmonic suppression scheme for full speed range of a two-level inverter fed induction motor drive using switched capacitive filter," IEEE Trans. Power Electron., vol. 32, no. 3, pp. 2064–2071, 2017.

[25] J. Druant, F. De Belie, P. Sergeant, and J. Melkebeek, "Field-Oriented Control for an Induction-Machine-Based Electrical Variable Transmission," IEEE Trans. Veh. Technol., vol. 65, no. 6, pp. 4230–4240, 2016.

[26] H. Echeikh, R. Trabelsi, A. Iqbal, N. Bianchi, and M. F. Mimouni, "Comparative study between the rotor flux oriented control and non-linear backstepping control of a five-phase induction motor drive - an experimental validation," IET Power Electron., vol. 9, no. 13, pp. 2510–2521, 2016.

[27] S. Chacko, C. N. Bhende, S. Jain, and R. K. Nema, "Rotor resistance estimation of vector controlled induction motor drive using GA/PSO tuned fuzzy controller," Int. J. Electr. Eng. Informatics, vol. 8, no. 1, pp. 218–236, 2016.

[28] S. K. Sahoo and T. Bhattacharya, "Rotor Flux-Oriented Control of Induction Motor with Synchronized Sinusoidal PWM for Traction Application," IEEE Trans. Power Electron., vol. 31, no. 6, pp. 4429–4439, 2016.

[29] S. Yang, D. Ding, X. Li, Z. Xie, X. Zhang, and L. Chang, "A Novel Online Parameter Estimation Method for Indirect Field Oriented Induction Motor Drives," IEEE Trans. Energy Convers., vol. 32, no. 4, pp. 1562–1573, 2017.

[30] Y. Zou, J. Li, X. Hu, and Y. Chamaillard, "Modeling and Control of Hybrid Propulsion System for Ground Vehicles," Model. Control Hybrid Propuls. Syst. Gr. Veh., pp. 23–51, 2018.